Amino Acids (2015) 47:1035–1043
DOI 10.1007/s00726-015-1935-z

ORIGINAL ARTICLE

Real-time heterogeneous protein–protein interaction between αA-crystallin N-terminal mutants and αB-crystallin using quartz crystal microbalance (QCM)

Srinivasagan Ramkumar · Noriko Fujii · Hiroaki Sakaue · Norihiko Fujii · Bency Thankappan · Rasiah Pratheepa kumari · Kalimuthusamy Natarajaseenivasan · Kumarasamy Anbarasu

Received: 31 May 2014 / Accepted: 4 February 2015 / Published online: 19 February 2015

Abstract The lens transparency depends on higher concentration of lens proteins and their interactions. α-Crystallin is one of the predominant lens proteins, responsible for proper structural and functional architecture of the lens microenvironment, and any alteration of which results in cataract formation. The R12C, R21L, R49C and R54C are the most significant and prevalent αA-crystallin congenital cataract-causing mutants worldwide. Protein–protein interaction, crucial for lens proper structure and function, was posited to be lost due to point mutation and the elucidation of which could shed light on the molecular basis of cataract. In this conjuncture, we report quartz crystal microbalance (QCM) as a warranted technique for real-time analysis of protein–protein interaction between the N-terminal mutants of αA-crystallin and αB-crystallin. The biophysical characteristics of the mutated proteins were determined by size-exclusion HPLC, far-UV circular dichroism and fluorescence studies. Far-UV circular dichroism spectral analysis displayed slight modifications in β-sheet of R54C mutant. Altered intrinsic tryptophan fluorescence and decreased bis-ANS fluorescence were observed in all the N-terminal mutations revealing the tertiary structural changes and decreased exposure of surface hydrophobicity. An emphatic fall in the chaperone activity was observed in the N-terminal mutants, R12C, R21L and R54C. QCM analysis revealed the occurrence of strong heterogeneous interaction between αA-crystallin and αB-crystallin. Nevertheless, decreased interactions were observed with the N-terminal mutants. In summary, the present study concludes that the loss of interactions between αA-crystallin N-terminal mutants and αB-crystallin signifies quaternary structural alterations due to mutation in the arginine residues.

Keywords Congenital cataract · αA-crystallin · Protein–protein interaction · QCM · Chaperone activity

Handling Editor: P. Kursula.

Electronic supplementary material The online version of this article (doi:10.1007/s00726-015-1935-z) contains supplementary material, which is available to authorized users.

S. Ramkumar · B. Thankappan · R. P. kumari · K. Anbarasu (✉)
Department of Marine Biotechnology, Bharathidasan University, Tiruchirappalli 620 024, Tamil Nadu, India
e-mail: anbumbt@bdu.ac.in

N. Fujii · H. Sakaue · N. Fujii
Research Reactor Institute, Kyoto University, Kumatori-cho, Sennan-gun, Osaka 590 0494, Japan

Present Address:
N. Fujii
Teikyo University, Itabashi, Japan

K. Natarajaseenivasan
Department of Microbiology, School of Life Sciences, Bharathidasan University, Tiruchirappalli 620 024, Tamil Nadu, India

Introduction

Human eye lens is typically hoarded by stable structural proteins called crystallins that are classified into three groups namely α-, β- and γ-crystallins, among which α-crystallin is expressed predominately for about 40 % of dry weight. α-crystallin subsists as oligomers at a molecular weight range of 200–800 kDa that casts high molecular weight aggregates during aging (Groenen et al. 1994). α-crystallin comprises two associated subtypes, αA- and αB-crystallin encoded by *CRYAA* and *CRYAB* genes into 173 and 175 amino acids, respectively, existing as an

oligomeric complex in the ratio of 3:1 (Ingolia and Craig 1982) with about 59 % sequence homologous. αA- and αB-crystallin being members of small heat shock protein family (Horwitz 1992) exert chaperone activity, a vital role taking part in both refraction and maintaining lens transparency.

Mutations in αA-crystallin have been evidenced to provoke congenital cataract, among which the reported, R12C (Hansen et al. 2007), R21L (Graw et al. 2006), R49C (Mackay et al. 2003) and R54C (Xia et al. 2006) are core mutations, since the residue in the N-terminal domain is accountable for oligomer formation and structural stability (Kundu et al. 2007). Moreover, it alters the homooligomeric or heterooligomeric complex with α-crystallin proteins implying the formation of large aggregate and aggresome, disrupting protein–protein interaction in live cells (Raju and Abraham 2011; Raju et al. 2012). Protein–protein interaction is the fundamental phenomenon of signal transduction in many biological activities that ascertain the light refraction, transparency and chaperone activity in the lens proteins (Ponce et al. 2006). A plethora of in vitro and in vivo techniques such as FRET, two-hybrid system and co-immunoprecipitation are reported for determining the lens proteins interaction (Siezen and Owen 1983; Liang and Li 1991; Koenig et al. 1992; Kumarasamy and Abraham 2008; Fujii et al. 2008; Raju et al. 2011, 2012; Chen et al. 2011; Kannan et al. 2013).

In this study, a real-time and highly sensitive, quartz crystal microbalance (QCM) assay was employed to demonstrate the protein–protein interaction between α-crystallin proteins. QCM is a label-free versatile technique employed to study protein–protein interactions in real time even at nanogram level (Roederer and Bastiaans 1983), which is based on changes in the resonance frequency of the piezoelectric quartz crystal. QCM is employed in a wide variety of fields including immunology, medicine and cell biology (Marx 2003; Chen et al. 2012; Reuel et al. 2012; Speight and Cooper 2012). Meanwhile, there is no report on application of QCM for studying protein–protein interaction of lens crystallin. Hence, the present study was aimed to study the biophysical characterization of human αA-crystallin and N-terminal mutants R12C, R21L, R49C and R54C as well as quantification of inter subunit interaction by QCM.

Materials and method

Materials

Molecular biology grade chemicals were purchased from Sigma Aldrich (St. Louis, MO, USA), Himedia (Mumbai, India) and Invitrogen. Q Sepharose XL and Sephacryl 300HR were purchased from Amersham Biosciences (Piscataway, NJ, USA), QuickChange II XL site-directed mutagenesis kit from Agilent Technologies Inc (CA, USA), and Affinix QCM immobilization kit from Initium Inc. (Japan).

Site-directed mutagenesis

Cloning of human recombinant αA- and αB-crystallin wild type (wt) in pET 3d and pET 23d(+) expression vectors, respectively, have been described earlier (Fujii et al. 2008). αA-crystallin N-terminal mutants such as R12C, R21L, R49C and R54C were created by QuickChange II XL site-directed mutagenesis kit following the manufacture protocol (Agilent Technologies Inc, CA, USA). Suitable mutagenic primers for αA-crystallin N-terminal mutants were designed manually by replacing a single nucleotide at the middle of the primer sequence. Thus, the resulting custom-synthesized primers (R12C, R21L, R49C and R54C) at Bioserve Biotechnologies (Hyderabad, India) have cysteine and leucine in the place of arginine as shown in Table 1. αA-crystallin wt was used as template to create the N-terminal mutants using PCR with the following conditions: initial denaturation at 95 °C for 1 min followed by 95 °C for 50 s, annealing at 60 °C for 50 s and extension at 68 °C for 5 min for 16 cycles, followed by overall extension at 68 °C for 7 min and kept at 4 °C. The PCR product was digested with *Dpn*I enzyme for 1 h at 37 °C and transformed into *E.coli* XL-10 Gold competent cells. Transformed cells were selected on LB agar plate containing 50 μg/ml ampicillin. All the mutants were confirmed by DNA sequencing.

Overexpression and purification of α-crystallin wt and αA-crystallin N-terminal mutants

Human αA-crystallin wt, N-terminal mutants and αB-crystallin in pET 3d and pET23d vector, respectively,

Table 1 List of custom-synthesized primers used for construction of αA-crystallin N-terminal mutants by site-directed mutagenesis method

αA-crystallin mutants	Forward primer	Reverse primer
R12C	TGGTTCAAG**T**GCACCCTGGGG	CCCCAGGGTGC**A**CTTGAACCA
R21L	TTCTACCCCAGCC**T**GCTGTTCGAC	GTCGAACAGC**A**GGCTGGGGTAGAA
R49C	CCCTACTAC**T**GCCAGTCCCTCT	AGAGGGACTGGC**A**GTAGTAGGG
R54C	TCCCTCTTC**T**GCACCGTGCTG	CAGCAGGGTGC**A**GAAGAGGGA

The bold letters represent the base pair changed for creation of site-directed mutants

were transformed into *E. coli* BL21 (DE3) pLysS cells. Protein production was induced by addition of 0.3 mM IPTG (isopropyl-1-thio-β-d-galactopyranoside). Cells were subsequently thawed, sonicated (6 rounds of 8 pulses per min) in 20 mM Tris–HCl, pH 7.8 containing 1 mM EDTA and 1 mM PMSF (phenylmethanesulfonyl fluoride). The sonicated products were centrifuged at 20,000 rpm for 20 min and the soluble fraction was subjected to ion exchange column chromatography on a Q Sepharose XL column (Amersham Biosciences, Piscataway, NJ) equilibrated with 20 mM Tris–HCl containing 1 mM EDTA and connected to an AKTA prime plus (GE Healthcare). Protein was eluted using a gradient of NaCl (0–1 M), with a flow rate of 10 ml/min. αA-crystallin wt and N-terminal mutants were eluted in 300 mM NaCl and αB-crystallin in 160 mM. Further, purification was achieved on a size-exclusion column (Sephacryl 300HR, Amersham Biosciences, Piscataway, NJ) equilibrated with 20 mM Tris–HCl pH 7.8 containing 150 mM NaCl. The purity of the recombinant proteins was checked using 15 % acrylamide gel. The purified αA-crystallin wt, N-terminal mutants and αB-crystallin wt were dialyzed against 50 mM sodium phosphate buffer at pH 7.8 for further biophysical experiments.

Size-exclusion chromatography

Molecular mass difference between αA-crystallin wt and N-terminal mutants was determined by size-exclusion chromatography using HPLC on TSKgel-G4000SWXL column (7.8 × 300 mm Tosho, Tokyo, Japan) equilibrated with 50 mM Tris/HCl containing 150 mM NaCl with the flow rate of 0.8 ml/min. 1 mg/ml of protein in 100 µl was injected onto the column and elution was monitored at 280 nm. Molecular mass of the proteins was calibrated with standards.

Secondary structure studies

Secondary structural variations between αA-crystallin wt and N-terminal mutants were determined using Jasco 810 spectropolarimeter, in the far-UV region of 195–250 nm. A cylindrical quartz cell with 1 mm path length and protein concentration of 0.1 mg/ml was used. Spectra were scanned for average of five times, corrected with buffer blank and smoothened prior to examination. The resultant spectra were analyzed for secondary structure by CDNN program.

Tryptophan fluorescence

The intrinsic tryptophan fluorescence spectra of αA-crystallin wt and N-terminal mutants were analyzed using an F-4500 Hitachi Fluorescence spectrophotometer (Hitachi, Tokyo, Japan). Respective protein samples (0.1 mg/ml) in 50 mM sodium phosphate buffer (pH 7.8) were excited at 295 nm and emission spectra collected at 300–400 nm.

Surface hydrophobicity

Surface hydrophobicity of αA-crystallin wt and N-terminal mutants was determined using the hydrophobic probe bis-ANS as described earlier (Fujii et al. 2008). Briefly, an aliquot of 100 µl of bis-ANS (0.1 mg/ml) was added to 100 µl of protein (1 mg/ml) along with 800 µl of 50 mM sodium phosphate buffer (pH 7.8). Prior to the experiment the mixture was kept in the dark condition for 15 min at room temperature. Florescence intensity was measured using F-4500 Hitachi fluorescence spectrophotometer (Hitachi, Tokyo, Japan) with excitation at 390 nm and emission at 460–540 nm.

Chaperone activity

Chaperone activities of αA-crystallin wt and N-terminal mutants were measured via the ability of the protein to protect alcohol dehydrogenase (ADH) from aggregation induced by EDTA with αA-crystallin and ADH in 1:5 ratio (w/w). Aliquot (500 µl) of 0.5 mg/ml ADH and 350 µl of 50 mM sodium phosphate buffer (pH 7.2) containing 100 mM NaCl were incubated for 30 min at 37 °C with 50 µl of respective crystallins (1.0 mg/ml). ADH aggregation was initiated by finally adding 100 µl of 100 mM EDTA to each of the incubated reaction mixtures in a thermostat holder of UV–Vis spectrophotometer (Shimadzu UV-1200, Kyoto, Japan); light scattering was monitored for 60 min at 360 nm and compared at the end. The data were statistically analyzed by one-way ANOVA using SPSS software and significance was considered at the level of $^{*}p < 0.05$ and $^{\#}p < 0.01$.

Quartz crystal microbalance (QCM)

Real-time interactions between αA-crystallin wt and N-terminal mutants with αB-crystallin wt were analyzed using 27 MHz QCM, (AFFINIX QNµ, Initium Inc., Japan). For this experiment, the protein immobilized on the sensor chip serves as ligand and the protein used for interaction study serves as analyte. The ligand was immobilized using affinity immobilization kit following manufacturer's protocol (Affinix QCM immobilization kit, Initium Inc., Japan).

Immobilization of ligand in sensor chip

The recombinant αB-crystallin wt was immobilized on gold-coated sensor chip by amine coupling method using 1-ethyl-3-(3-dimethylaminopropyl)-carbodiimide

hydrochloride (EDC) and N-hydroxysuccinimide (NHS). For immobilization, 1 mg/ml of αB-crystallin was diluted to 100 µg/ml using the appropriate buffer at pH 5.0 following manufacturer's protocol.

Initially, quartz crystal was cleaned with 1 % SDS followed by 3 µl piranha solution (3:1 ratio of sulfuric acid and hydrogen peroxide) for 5 min and finally by milliQ water. The sensor surface was pre-activated with 50 µl COOH-SAM for 1 h and washed by milliQ water. Then, 50 µl of EDC/NHS mix at the ratio of 1:1 was injected over the sensor chip for 15 min to activate carboxyl group on the sensor surface. Excess EDC/NHS solution was removed by milliQ water. Sensor chip was flooded with 100 µg/ml of αB-crystallin wt and allowed to stay for 15 min. The remaining active sites were blocked by adding 100 µl of ethanolamine for 30 min. The unbounded αB-crystallin was removed with 50 µl of 3 M guanidine HCl for 30 s and finally washed with milliQ water. The quantity of αB-crystallin bounded on the sensor chip was 18 ng.

Examination of interaction between immobilized ligands with analyte

αA-crystallin wt at a final concentration of 100 µg/ml (analyte) in PBS (pH 7.4) was used to quantify the interaction in real time. The analyte was passed over the sensor chip containing immobilized αB-crystallin wt and the binding efficacy was monitored by frequency logging for 600 s, and the resulting frequency shifts were recorded and evaluated by AQUA SOFTWARE. Similar procedure was employed for analyzing the N-terminal mutants with αB-crystallin wt. The control flow was carried out by passing the analyte in the sensor chip without immobilized ligand. The experiment was repeated for five times and the data were statistically analyzed by one-way ANOVA using SPSS software and significance was considered at the level of $^{*}p < 0.05$ and $^{\#}p < 0.01$.

Results

Protein purification

Purity of each recombinantly produced α-crystallins was checked by SDS-PAGE (Supplementary Fig. 1A, B). A single, clear and distinct band at 20.1 kDa indicated the purity of the proteins.

Size-exclusion HPLC

The size-exclusion chromatographic profile of αA-crystallin wt and N-terminal mutants is shown in Fig. 1a. The results demonstrate that mutants eluted slightly earlier than wt counterparts indicating the increased molecular mass due to aggregation. The elution profile shows that molecular mass of R12C was slightly higher followed by R54C, R49C, R21L and αA-crystallin wt.

CD spectroscopy

The secondary structure profile of αA-crystallin wt and N-terminal mutated proteins is shown in Fig. 1b. The negative ellipticity at 218 and 206 nm indicates the predominant β-sheet structure of α-crystallin protein (Table 2). CD spectra of the N-terminal mutants showed no/slight change in the secondary structure of R12C, R21L and R49C mutants, and slight loss was observed in the β-sheet content of R54C mutant when compared with its wt counterpart.

Tryptophan fluorescence

Tertiary structural features of the αA-crystallin wt and N-terminal mutants were assessed by tryptophan fluorescence. The assay is based on the presence of aromatic amino acid tryptophan at the surface of αA-crystallin protein. Fluorescent intensity was decreased in the N-terminal mutants R12C, R21L and R54C when compared with the αA-crystallin wt (Fig. 1c). However, the mutant R49C exhibited increased fluorescence intensity depicting alteration of aromatic residues exposed in the surface of the protein. The increase or decrease of intrinsic tryptophan fluorescence emission at 338 nm in the N-terminal mutants illustrates variations in the physical structure of the protein from their wt counterpart.

Surface hydrophobicity

Bis-ANS was used to monitor the exposed surface hydrophobicity of αA-crystallin. This hydrophobic probe binds with hydrophobic surface of the protein, wherein the emission intensity is enhanced upon binding. Significant difference in the intensity was observed in the αA-crystallin wt and N-terminal mutants. The N-terminal mutated proteins demonstrated a remarkable decrease in fluorescence intensity compared to αA-crystallin wt (Fig. 1d).

Chaperone activity

Chaperone activity of αA-crystallin wt and N-terminal mutants was determined using ADH as target protein in the ratio of 1:5. Both αA wt and R49C exhibited 92 and 87 %, respectively, in the suppression of ADH aggregation induced by EDTA, whereas other mutants showed progressive decrease in chaperone activity in the following order of percentages, R54C—75 % > R21L—72 % > R12C—42 % (Fig. 1e, f). The result reveals that all the mutations

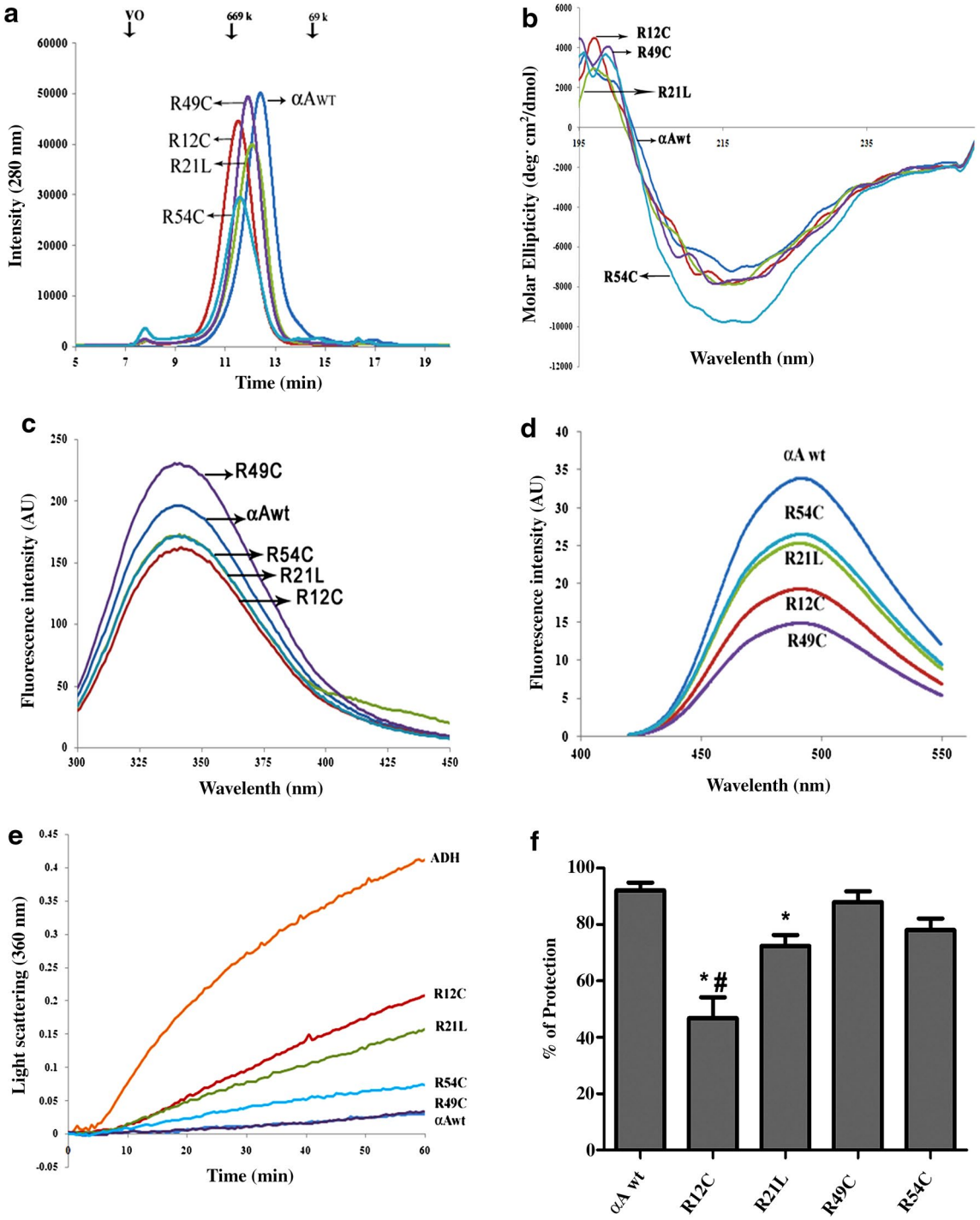

Fig. 1 **a** Size-exclusion HPLC spectrum of αA-crystallin wt and N-terminal mutants. The Vo represents the void volume and the elution profile of mass standards were thyroglobulin (669 kDa) and bovine serum albumin (69 kDa). **b** The secondary structural difference between αA-crystallin wt and N-terminal mutants (R12C, R21L, R49C and R54C) determined in the far-UV region of 195–250 nm. **c** The intrinsic tryptophan fluorescence spectra of αA-crystallin wt and N-terminal mutants (R12C, R21L, R49C and R54C). **d** Surface hydrophobicity of αA-crystallin wt and N-terminal mutants determined using bis-ANS probe. **e** Chaperone activity of αA-crystallin wt and N-terminal mutants analyzed by EDTA-induced aggregation of alcohol dehydrogenase (ADH). **f** Bar diagram represents the summary of chaperone activity data from three independent experiments. Each bar represents the mean ± SD. $^{*}p < 0.05$, $^{\#}p < 0.01$ (compared to lane 1 in each case)

Table 2 The far-UV CD spectra of αA-crystallin wt and N-terminal mutants were quantitatively analyzed by CDNN software

Protein	Percentage (%)			
	α-Helix	β-Sheet	β-Turn	Random coil
αA-wt	18.9	30.7	16.4	33.7
R12C	18.8	30.5	16.1	34.3
R21L	18.7	30.7	16.4	33.9
R49C	19.6	30.2	16.5	32.9
R54C	21.9	27.9	16.8	33.1

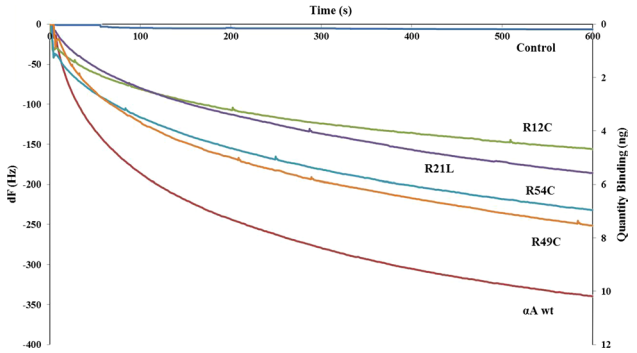

Fig. 2 Real-time heterogeneous interaction of αA-crystallin wt and N-terminal mutants with αB-crystallin wt. Differential interaction of αA-crystallin wt and N-terminal mutants with native αB-crystallin was analyzed using 27 MHz Quartz crystal microbalance (QCM) (AFFINIX QN, Japan). The sensogram where αB-crystallin wt was immobilized and acts as a ligand and αA-crystallin wt and N-terminal mutants were used as analytes in a separate experiment, and binding quantity was analyzed by AQUA software. The results show that αA-crystallin and αB-crystallin wt interacts strongly showing a decrease in frequency values up to −350 Hz which is directly proportional to the binding quantity of 10.5 ng and very low interaction was observed in the mutant R12C with −150 Hz and binding quantity of 4.9 ng followed by the mutant R21L with −170 Hz and binding quantity of 5.7 ng, R54C with −200 Hz and binding quantity of 7.1 ng, R49C with −220 Hz and binding quantity of 7.5 ng. The control is the frequency of basal run without binding of ligand

in the N-terminal region do not follow similar pattern of chaperone activity, which mainly depends on the position of mutation.

Real-time interaction analysis with QCM

Real-time heterogeneous interaction of αA-crystallin wt and N-terminal mutants with αB-crystallin wt was determined by QCM. Figure 2 sensogram represents the binding efficiency of αA-crystallin wt and N-terminal mutant subunits with immobilized αB-crystallin wt in terms of decreasing frequency. The frequency of interaction between αA-crystallin wt and αB-crystallin wt was 100 %. However, the interaction of the N-terminal mutants with αB-crystallin wt was comparatively lower, R54C—61.9 %, R49C—61.5 %, R21L—55.8 % and R12C—41 %. The mean ± SD of five individual experiments to determine the frequency logging due to increase in mass for αA-crystallin wt and N-terminal mutants with αB-crystallin wt are given as Supplementary Fig. 2 and quantitative binding analysis performed with AQUA software results as Supplementary Fig. 3.

Discussion

In the human eye, lens protein–protein interaction plays a significant role to generate a gradient of refractive index in the fiber cells, so that light can be specially focused to the retina without scattering (Evgrafov et al. 2004). It was reported that a decrease in protein–protein interaction between α-crystallin and other proteins may underlie the formation of cataract (Fu and Liang 2002; Liang 2004; Kumarasamy and Abraham 2008; Raju and Abraham 2011; Raju et al. 2012). Earlier αA-crystallin knockout studies demonstrated stabilization of αB-crystallin by αA-crystallin suggesting that αB-crystallin synthesized in the absence of αA-crystallin forms large inclusion bodies (Brady et al. 1997) revealing the importance of heteroaggregate formation of αA- and αB-crystallin in maintaining lens transparency. Hence, in this study we have focused on heterogeneous interaction rather than homogeneous interaction among the α-crystallins.

Homogeneous and heterogeneous interactions of α-crystallins have been demonstrated by a number of in vitro and in vivo methods such as light scattering (Mach et al. 1990), florescence polarization (Liang and Li 1991), fluorescence resonance energy transfer (Bova et al. 2002; Liang and Liu 2006; Kumarasamy and Abraham 2008), surface plasmon resonance (Peterson et al. 2005), microequilibrium dialysis (Ponce and Takemoto 2005), etc. In spite of various advantages and disadvantages associated with each aforesaid technique, a real-time and quantitative interaction analysis is warranted. Hence in the present study, the interactions between α-crystallins were studied by QCM analysis. To the best of our knowledge, there is no previous report available to determine the α-crystallin interactions using QCM as a tool.

Quartz crystal microbalance results suggest that interaction of αA-crystallin with αB-crystallin was quite stronger as indicated by decrease in frequency level up to −350 df (Hz), reflecting the formation of strong heteroaggregates. However, the frequency of all the mutants was significantly elevated when compared with wild type. The increase in interaction frequency of the mutants indicates reduced interaction, manifesting the loss of heteroaggregate formation potential of αA-crystallin due to point mutation. Due to the loss of interaction between N-terminal mutants

of αA-crystallin, the αB-crystallin is incapable of fully protecting αA-crystallin mutants from forming insoluble aggregates suspected to be the underlying cause for cataract formation in early age as described earlier (Raju et al. 2012). In addition, it also strongly augments understanding of the importance of positively charged arginine residue in the 12th, 21st, 49th and 54th N-terminal residues which has been mutated to neutral residue. Previous literature suggests that arginine in the αA-crystallin N-terminal region of aforesaid position is crucial for forming salt bridges with neighboring negatively charged residues eventually leading to homo- and heteroaggregate formation thereby maintaining lens transparency (Shroff et al. 2000; Cobb and Petrash 2000; Andley et al. 2002; Bera et al. 2002; Hsu et al. 2006; Kore et al. 2012).

In addition to interaction analysis, the biophysical characteristics of recombinant αA-crystallin wt and N-terminal mutants were also evaluated. The oligomeric size of the mutants was slightly increased when compared with its wt counterparts. The mutant, R12C eluted foremost followed by R54C, R21L, R49C and αA-crystallin wt. Elution profile illustrates that N-terminal domain is essential for maintaining the oligomeric size and the point mutants evaluated in this study are suspected to be aggregated leading to slightly increased oligomeric size. However, except for R12C, other mutants did not show any considerable variation in elution profile and go in line with previous reports of Kore et al. (2012) in which the molar mass, hydrodynamic radius and polydispersity index of the mutants were analyzed using dynamic light-scattering measurements. Contrastingly, the oligomeric size formation due to mutation at 116th residue conversion of arginine to cysteine is substantially significant than the N-terminal domain mutations, since about 4- to 10-fold increases in oligomeric size were observed in a study done by Andley et al. (2002). Many researchers have reported that replacement of cys residues results in formation of disulfide bonds that result in dimerization which reflects in the interactive nature of α-crystallin. In this study, we have focused on the extent of interaction between the αA-crystallin wild type and selected N-terminal mutants. Earlier we have reported that mutation in arginine to cysteine conversion enhances cross-linked product formation when compared with the leucine conversion as well as the formation of disulfide bond between intra- or inter-polypeptide (Ramkumar et al. 2013). Hence due to these disulfide bond formation leads to random oligomerization of protein thereby the hydrophobic patches are buried deep within (Kore et al. 2012). As a result the surface hydrophobicity of the mutant proteins is drastically reduced/altered, as when compared to the wild type αA-crystallin leads to change their structural confirmation as well as functional characteristics.

The prime secondary structure of α-crystallin is β-sheet. Even though, no significant secondary structural changes were noticed between the αA-crystallin wt and mutants, slight loss in the beta-sheet content of the mutant R54C was indeed observed. The percentages of secondary structural contents of all the mutants are listed in Table 2. The possible reason for the loss of β-sheet and increased α-helix (3 %) may be due to the substrate binding ability of the 54th amino residue. However, noticeable tertiary structural changes in the mutants were observed corroborating with the previous findings of Kore et al. (2012). The tertiary structural changes measured by tryptophan fluorescence revealed that except R49C, the fluorescence intensity of all the N-terminal mutants was decreased, which could be the underlying rationale for structural perturbations leading to altered tryptophan microenvironment in all the mutant proteins. Fall in tryptophan fluorescence reveals that the residue is more water exposed referable to the conformational changes in the N-terminal region. But, strikingly R49C mutation results in protein tertiary structural alteration that propelled the exposure of tryptophan residue. Changes in secondary and tertiary structures could potentially alter the exposure of hydrophobic residues. A scale down in surface hydrophobic patches was observed in all the mutant proteins substantiating the structural perturbations rendered due to the respective point mutations. These findings exhibited a slight deviation from the previous report of Kore et al. (2012), in which all the mutants demonstrated reduced fluorescence intensity, except R21W and R21L. This discrepancy in the results may be due to the difference of hydrophobic probe employed. Bis-ANS strongly interacts with monomeric A-state and the unfolded monomers of the proteins.

Many studies testified that α-crystallin is a better chaperone protein with potential to prevent other target proteins from aggregation during unfavorable environmental conditions thereby avoiding cataract formation in eye lens. For determination of α-crystallin chaperone activity, a number of target proteins were employed such as bovine lens β_L-crystallin, insulin, ADH, γD-crystallin and citrate synthase in different ratios, induced with different reagents (Wang and Spector 2001; Kumarasamy and Abraham 2008). The results are highly controversial and depend on the ratio of crystallin and target proteins used, reducing agent and temperature. Selection of an appropriate target protein and optimum temperature is the crucial factors for this sort of in vitro experiments. Recently, Kore et al. (2012) employed EDTA to induce aggregation of ADH as substrate protein at 37 °C for chaperone assay and established the protocol to be highly reproducible, and hence we relied on the method. Among the four mutants, three mutants R12C, R21L and R54C showed loss of chaperone activity suggesting that the arginine at the 12th, 21st, 54th positions in the N-terminal

end is critical for the chaperone activity of the αA-crystallin validating earlier findings (Kore et al. 2012).

The magnitude of the increase in chaperone activity is less than the increase in bis-ANS binding by R49C, because the hydrophobic probes such as bis-ANS also interact at regions that do not contribute to chaperone-like function (Sharma et al. 1998). The specific correlation between the surface hydrophobic residues and chaperone activity is yet to be elucidated; nevertheless, many researchers have addressed a strong negative correlation between surface hydrophobicity and chaperone activity (Santhoshkumar and Sharma 2001; Bhattacharyya et al. 2002; Kumar et al. 2005; Reddy et al. 2006; Wang et al. 2007).

The present study illustrates that the αA-crystallin N-terminal mutations at 12th, 21st, 49th and 54th positions may be responsible for distortion in the biophysical characterization of the proteins as well as interactive potential with αB-crystallin. However, it is not ultimate that all the examined mutants undergo similar alterations and might depend on the actual position of the mutation occurred. We believe our report to be the first to undertake QCM for crystallin interaction studies with αA-crystallin N-terminal mutants and αB-crystallin. The results not only illustrate the interaction between crystallins but also introduce a better sensitive and reliable real-time technique for in vitro protein–protein interaction.

Acknowledgments The authors gratefully acknowledge the financial assistance from Department of Science and Technology (DST), New Delhi as DST-YS (SR/FT/LS-153/2008/(2010–2013) and DST-JSPS—Indo-Japan co-operative collaboration project (DST/INT/JSPS/P-119/(2011–2013) sanctioned to the corresponding author (Dr. KA). The 5th and 6th authors thank DST-INSPIRE and DST-PURSE for fellowship.

Conflict of interest The authors have no conflicts to declare.

References

Andley UP, Patel HC, Xi J-H (2002) The R116C mutation in alpha A-crystallin diminishes its protective ability against stress-induced lens epithelial cell apoptosis. J Biol Chem 277:10178–10186

Bera S, Thampi P, Cho WJ, Abraham EC (2002) A positive charge preservation at position 116 of alpha A-crystallin is critical for its structural and functional integrity. Biochemistry 41:12421–12426

Bhattacharyya J, Srinivas V, Sharma KK (2002) Evaluation of hydrophobicity versus chaperonelike activity of bovine alphaA- and alphaB-crystallin. J Protein Chem 21:65–71

Bova MP, Huang Q, Ding L, Horwitz J (2002) Subunit exchange, conformational stability, and chaperone-like function of the small heat shock protein 16.5 from *Methanococcus jannaschii*. J Biol Chem 277:38468–38475

Brady JP, Garland D, Duglas-Tabor Y, Robison WG Jr, Groome A, Wawrousek EF (1997) Targeted disruption of the mouse alpha A-crystallin gene induces cataract and cytoplasmic inclusion bodies containing the small heat shock protein alpha B-crystallin. Proc Natl Acad Sci USA 94:884–889

Chen Y-H, Lee M-T, Cheng Y-W, Chou W-Y, Yu C-M, Lee H-J (2011) Distinct interactions of αA-crystallin with homologous substrate proteins, δ-crystallin and argininosuccinate lyase, under thermal stress. Biochimie 93:314–320

Chen Y-LS, Li J-H, Yu C-Y, Lin C-J, Chiu P-H, Chen P-W, Lin C-C, Chen W-J (2012) Novel cationic antimicrobial peptide GW-H1 induced caspase-dependent apoptosis of hepatocellular carcinoma cell lines. Peptides 36:257–265

Cobb BA, Petrash JM (2000) Structural and functional changes in the alpha A-crystallin R116C mutant in hereditary cataracts. Biochemistry 39:15791–15798

Evgrafov OV, Mersiyanova I, Irobi J, Van Den Bosch L, Dierick I, Leung CL, Schagina O, Verpoorten N, Van Impe K, Fedotov V, Dadali E, Auer-Grumbach M, Windpassinger C, Wagner K, Mitrovic Z, Hilton-Jones D, Talbot K, Martin JJ, Vasserman N, Tverskaya S, Polyakov A, Liem RKH, Gettemans J, Robberecht W, De Jonghe P, Timmerman V (2004) Mutant small heat-shock protein 27 causes axonal Charcot–Marie–Tooth disease and distal hereditary motor neuropathy. Nat Genet 36:602–606

Fu L, Liang JJ-N (2002) Detection of protein-protein interactions among lens crystallins in a mammalian two-hybrid system assay. J Biol Chem 277:4255–4260

Fujii N, Hisano T, Fujii N (2008) Study of subunit interactions of alpha A- and alpha B-crystallins and the effects of gamma-irradiation on their interactions by surface plasmon resonance. Biochim Biophys Acta 1784:1507–1513

Graw J, Klopp N, Illig T et al (2006) Congenital cataract and macular hypoplasia in humans associated with a de novo mutation in CRYAA and compound heterozygous mutations in P. Graefes Arch Clin Exp Ophthalmol 244:912–919

Groenen PJ, Merck KB, de Jong WW, Bloemendal H (1994) Structure and modifications of the junior chaperone alpha-crystallin. From lens transparency to molecular pathology. Eur J Biochem 225:1–19

Hansen L, Yao W, Eiberg H, Kjaer KW, Baggesen K, Hejtmancik JF, Rosenberg T (2007) Genetic heterogeneity in microcornea-cataract: five novel mutations in CRYAA, CRYGD, and GJA8. Invest Ophthalmol Vis Sci 48:3937–3944

Horwitz J (1992) Alpha-crystallin can function as a molecular chaperone. Proc Natl Acad Sci U S A 89:10449–10453

Hsu C-D, Kymes S, Petrash JM (2006) A transgenic mouse model for human autosomal dominant cataract. Invest Ophthalmol Vis Sci 47:2036–2044

Ingolia TD, Craig EA (1982) Four small Drosophila heat shock proteins are related to each other and to mammalian alpha-crystallin. Proc Natl Acad Sci USA 79:2360–2364

Kannan R, Santhoshkumar P, Mooney BP, Sharma KK (2013) Identification of subunit-subunit interaction sites in αA-WT crystallin and mutant αA-G98R crystallin using isotope-labeled cross-linker and mass spectrometry. PLoS One 8:e65610

Koenig SH, Brown RD, Spiller M, Chakrabarti B, Pande A (1992) Intermolecular protein interactions in solutions of calf lens alpha-crystallin. Results from 1/T1 nuclear magnetic relaxation dispersion profiles. Biophys J 61:776–785

Kore R, Hedges RA, Oonthonpan L, Santhoshkumar P, Sharma KK, Abraham EC (2012) Quaternary structural parameters of the congenital cataract causing mutants of αA-crystallin. Mol Cell Biochem 362:93–102

Kumar MS, Kapoor M, Sinha S, Reddy GB (2005) Insights into hydrophobicity and the chaperone-like function of alphaA- and alphaB-crystallins: an isothermal titration calorimetric study. J Biol Chem 280:21726–21730

Kumarasamy A, Abraham EC (2008) Interaction of C-terminal truncated human alphaA-crystallins with target proteins. PLoS One 3:e3175

Kundu M, Sen PC, Das KP (2007) Structure, stability, and chaperone function of alphaA-crystallin: role of N-terminal region. Biopolymers 86:177–192

Liang JJ-N (2004) Interactions and chaperone function of alphaA-crystallin with T5P gamma C-crystallin mutant. Protein Sci 13:2476–2482

Liang JN, Li XY (1991) Interaction and aggregation of lens crystallins. Exp Eye Res 53:61–66

Liang JJ, Liu B-F (2006) Fluorescence resonance energy transfer study of subunit exchange in human lens crystallins and congenital cataract crystallin mutants. Protein Sci 15:1619–1627

Mach H, Trautman PA, Thomson JA, Lewis RV, Middaugh CR (1990) Inhibition of alpha-crystallin aggregation by gamma-crystallin. J Biol Chem 265:4844–4848

Mackay DS, Andley UP, Shiels A (2003) Cell death triggered by a novel mutation in the alphaA-crystallin gene underlies autosomal dominant cataract linked to chromosome 21q. Eur J Hum Genet 11:784–793

Marx KA (2003) Quartz crystal microbalance: a useful tool for studying thin polymer films and complex biomolecular systems at the solution–surface interface. Biomacromolecules 4:1099–1120

Peterson J, Radke G, Takemoto L (2005) Interaction of lens alpha and gamma crystallins during aging of the bovine lens. Exp Eye Res 81:680–689

Ponce A, Takemoto L (2005) Screening of crystallin–crystallin interactions using microequilibrium dialysis. Mol Vis 11:752–757

Ponce A, Sorensen C, Takemoto L (2006) Role of short-range protein interactions in lens opacifications. Mol Vis 12:879–884

Raju I, Abraham EC (2011) Congenital cataract causing mutants of αA-crystallin/sHSP form aggregates and aggresomes degraded through ubiquitin-proteasome pathway. PLoS ONE 6:e28085

Raju I, Kumarasamy A, Abraham EC (2011) Multiple aggregates and aggresomes of C-terminal truncated human αA-crystallins in mammalian cells and protection by αB-crystallin. PLoS ONE 6:e19876

Raju I, Oonthonpan L, Abraham EC (2012) Mutations in human αA-crystallin/sHSP affect subunit exchange interaction with αB-crystallin. PLoS One 7:e31421

Ramkumar S, Fujii N, Fujii N, Thankappan B, Sakaue H, Ingu K, Natarajaseenivasan K, Anbarasu K (2013) Comparison of effect of gamma ray irradiation on wild-type and N-terminal mutants of αA-crystallin. Mol Vis 7(20):1002–1016

Reddy GB, Kumar PA, Kumar MS (2006) Chaperone-like activity and hydrophobicity of alpha-crystallin. IUBMB Life 58:632–641

Reuel NF, Mu B, Zhang J, Hinckley A, Strano MS (2012) Nanoengineered glycan sensors enabling native glycoprofiling for medicinal applications: towards profiling glycoproteins without labeling or liberation steps. Chem Soc Rev 41:5744–5779

Roederer JE, Bastiaans GJ (1983) Microgravimetric immunoassay with piezoelectric crystals. Anal Chem 55:2333–2336

Santhoshkumar P, Sharma KK (2001) Phe71 is essential for chaperone-like function in alpha A-crystallin. J Biol Chem 276:47094–47099

Sharma KK, Kumar GS, Murphy AS, Kester K (1998) Identification of 1,1′-bi(4-anilino)naphthalene-5,5′-disulfonic acid binding sequences in alpha-crystallin. J Biol Chem 273:15474–15478

Shroff NP, Cherian-Shaw M, Bera S, Abraham EC (2000) Mutation of R116C results in highly oligomerized alpha A-crystallin with modified structure and defective chaperone-like function. Biochemistry 39:1420–1426

Siezen RJ, Owen EA (1983) Interactions of lens proteins. Self-association and mixed-association studies of bovine alpha-crystallin and gamma-crystallin. Biophys Chem 18:181–194

Speight RE, Cooper MA (2012) A survey of the 2010 quartz crystal microbalance literature. J Mol Recognit 25:451–473

Wang K, Spector A (2001) ATP causes small heat shock proteins to release denatured protein. Eur J Biochem 268:6335–6345

Wang Y, Wang S-Y, Zhang X-H, Zhao M, Hou CM, Xu YJ, Du ZY, Yu XD (2007) FK228 inhibits Hsp90 chaperone function in K562 cells via hyperacetylation of Hsp70. Biochem Biophys Res Commun 356:998–1003

Xia C, Liu H, Chang B, Cheng C, Wang M, Huang Q, Horwitz J, Gong X (2006) Arginine 54 and Tyrosine 118 residues of {alpha} A-crystallin are crucial for lens formation and transparency. Invest Ophthalmol Vis Sci 47:3004–3010